Advances in Bioresearch
Adv. Biores., Vol 16 (5) September 2025: 33-54

Print ISSN 0976-4585; Online ISSN 2277-1573
Journal's URL:http://www.soeagra.com/abr.html
CODEN: ABRDC3
DOI: 10.15515/abr.0976-4585.16.5.3354

Advances in Bioresearch

ORIGINAL ARTICLE

Design, Optimization, and Evaluation of Liquid Self-Nanoemulsifying Drug Delivery System (L-SNEDDS) of 1,8-Cineole: Development into A Solid Capsule Dosage Form

Sayali A. Murtadak*, Raosaheb S. Shendge
Department of Pharmaceutics, Sanjivani College of Pharmaceutical Education and Research, Kopergaon, Savitribai Phule Pune University, 423601, Ahmadnagar, Maharashtra, India.
Corresponding Author E-mail: sayalimurtadak11@gmail.com

ABSTRACT
The present study was designed to develop, optimize, and evaluate a Liquid Self-Nanoemulsifying Drug Delivery System (L-SNEDDS) for 1,8-Cineole, a lipophilic monoterpene with known pharmacological activities but poor aqueous solubility and low oral bioavailability. The study also aimed to convert the optimized L-SNEDDS into a solid capsule dosage form to improve stability, patient compliance, and ease of administration. A comprehensive preformulation study was conducted using techniques such as FTIR, DSC, HPTLC, and boiling point analysis to confirm the identity and compatibility of 1,8-Cineole with excipients. Solubility screening and pseudo-ternary phase diagram construction were carried out to identify suitable oils, surfactants, and co-surfactants. Based on the findings, 1,8-Cineole, Tween 80, and PEG-200 were selected as key components. The formulation was optimized using Central Composite Design (CCD) within the framework of Response Surface Methodology (RSM). The optimized batch (F8) showed a droplet size of 110.3 nm, zeta potential of −17.54 mV, polydispersity index of 0.049, and a rapid in-vitro drug release of 89.83% within 60 minutes. To address limitations associated with the liquid system, the L-SNEDDS was solidified using lyophilization with mannitol and encapsulated. The resulting Solid SNEDDS (S-SNEDDS) capsules demonstrated excellent flow properties, uniform drug content (96.28%), and enhanced dissolution (95.90% in 60 minutes). Characterization through FTIR, DSC, SEM, and TEM confirmed structural integrity and compatibility. Stability studies conducted over 90 days confirmed the robustness of the final formulation. Overall, this study establishes a novel, scalable, and effective drug delivery platform for enhancing the oral bioavailability of 1,8-Cineole using SNEDDS technology.
Keywords: *1,8-Cineole; L-SNEDDS; Solid SNEDDS; Capsule; Bioavailability; Nanoemulsion; Central Composite Design; In-vitro release*

Received 27.04.2025 Revised 25.07.2025 Accepted 30.08.2025

How to cite this article:
Sayali A. M, Raosaheb S. S. Design, Optimization, and Evaluation of Liquid Self-Nanoemulsifying Drug Delivery System (L-SNEDDS) of 1,8-Cineole: Development into A Solid Capsule Dosage Form. Adv. Biores., Vol 16 (5) September 2025: 33-54.

INTRODUCTION

The oral route is the most preferred method for drug administration due to its convenience, cost-effectiveness, and patient compliance. However, a significant limitation arises when dealing with poorly water-soluble drugs, as their bioavailability is often low due to poor dissolution in gastrointestinal fluids. This issue has prompted the development of various strategies to enhance oral bioavailability, among which lipid-based formulations, particularly self-nanoemulsifying drug delivery systems (SNEDDS), have gained considerable attention (1–4).

SNEDDS are isotropic mixtures of oil, surfactant, and co-surfactant that spontaneously emulsify upon dilution in the gastrointestinal tract, forming fine oil-in-water nanoemulsions with droplet sizes typically less than 200 nm. These systems enhance drug solubilization, improve dissolution kinetics, and facilitate lymphatic absorption, thereby bypassing hepatic first-pass metabolism. Moreover, the nano-size droplets provide a large surface area for absorption, improving the pharmacokinetic profile of lipophilic drugs (5–7).

1,8-Cineole, also known as eucalyptol, is a naturally occurring monoterpene oxide found in various essential oils, including eucalyptus, rosemary, and bay leaves (8–10). It possesses a wide spectrum of pharmacological activities such as anti-inflammatory, mucolytic, bronchodilator, antimicrobial, and potential anticancer effects. Despite these benefits, the therapeutic application of 1,8-Cineole is hindered by its poor aqueous solubility, volatility, and instability under environmental conditions (11). To overcome these challenges, encapsulation into SNEDDS has been proposed as a promising approach to stabilize the compound, enhance its solubility, and improve systemic delivery.

Liquid SNEDDS (L-SNEDDS) formulations are advantageous in enhancing solubility and absorption of lipophilic drugs like 1,8-Cineole; however, they suffer from drawbacks such as leakage, instability, and difficulty in dosage uniformity. These challenges necessitate the conversion of L-SNEDDS into solid self-nanoemulsifying drug delivery systems (S-SNEDDS), which combine the solubility benefits of lipid-based systems with the physical and chemical stability of solid dosage forms. Solidification techniques such as lyophilization using cryoprotectants like mannitol offer a viable strategy for transforming L-SNEDDS into a robust, stable, and easily administrable solid form, including capsules (1,12–14).

The present study aims to design, optimize, and characterize a novel L-SNEDDS formulation of 1,8-Cineole and further develop it into a solid capsule dosage form. A systematic formulation approach involving excipient screening, pseudo-ternary phase diagram construction, and statistical optimization using Central Composite Design (CCD) was employed. The optimized formulation was subjected to extensive physicochemical characterization using techniques such as FTIR, DSC, particle size analysis, zeta potential, SEM, and TEM. Additionally, in-vitro release and stability studies were conducted to evaluate the performance and shelf-life of the final product. This research presents a comprehensive formulation strategy for enhancing the delivery of a bioactive but poorly soluble phytoconstituent, providing a promising platform for clinical translation of lipid-based delivery systems in phytopharmaceuticals.

MATERIAL AND METHODS

Materials

The materials used in the study were obtained from reputable suppliers to ensure quality and consistency. 1,8-Cineole, PEG 400, PEG 600, PEG 200, Tween 80, and Propylene Glycol were procured from Research-Lab Fine Chem. Industries. Olive oil, sunflower oil, castor oil, and 1,8-Cineole were sourced from Modern Industries, ensuring high-grade plant-based oils. Tween 20 was obtained from Loba Chemie. These materials, including oils and surfactants, were carefully selected for their suitability in the formulation and experimental processes.

Methods

Preformulation study

Preformulation study is the important and primary study in development of any dosage form. Preformulation is defined as an investigation of physical and chemical properties of the drug substance alone and with excipients. Hence, Preformulation study of the drug is useful to develop the stable formulation.

Identification and Confirmation of Drug

Identification and Confirmation of drug was carried out by boiling point method and DSC, FTIR, HPTLC methods.

Boiling Point Method

The boiling point of a liquid can be determined using a simple laboratory setup. A small volume of the liquid is placed in a boiling tube or test tube, along with a boiling chip to prevent bumping. The tube is then clamped in a vertical position and partially immersed in a liquid bath, such as water, oil, or paraffin, depending on the expected boiling point range. A thermometer is positioned so that its bulb is just above the surface of the liquid being tested, ensuring accurate measurement of the vapor temperature. The liquid bath is gently heated until a continuous stream of bubbles emerges from the liquid, indicating it is boiling. The temperature at which the liquid boils and maintains steady bubbling is recorded as its boiling point.

FTIR Spectroscopy

The pure 1,8-Cineole was taken liquid cells with appropriate window materials like KBr, an infrared transparent matrix at 1:100 (sample: KBr) ratio, respectively. The liquid cells were then scanned over a wave range of 4000 – 400 cm^{-1} and spectra was obtained by using a FTIR spectrometer-430 (Shimadzu 8400S, Japan) (15,16).

Differential Scanning Calorimetry

Thermogram for 1,8-Cineole was obtained using DSC (Mettler DSC 1star system, Mettler-Toledo, Switzerland). The drug was sealed in perforated aluminum pan and heated at constant rate of 10°C/min over the temperature ranges of -10-350°C at 20ml/min nitrogen purging (17,18).

Standard Calibration Curve in HPTLC

Method of Sample and Standard Solution's Preparation

Accurately measured 20 µL of standard eucalyptol was dissolved in methanol in a 10-mL volumetric flask to get a concentration of 184.50ng/µL. Different volumes of working standard, i.e., 0.5, 1, 2, 3, 4, 5, and 6µL, were applied on TLC.

Mobile Phase Selection

For the HPTLC analysis of eucalyptol, the best mobile phase is Toluene: Ethyl Acetate (9:1) provides optimal separation for non-polar to moderately polar terpenes. These mobile phases ensure good resolution, minimal tailing, and efficient migration on silica gel plates. Final optimization can be based on RF values and separation quality (19).

Instrumentation and Chromatographic Conditions

The HPTLC analysis of eucalyptol is carried out using pre-coated silica gel 60 F254 plates as the stationary phase. The sample is applied using an automatic sample applicator, such as the CAMAG Linomat 5, to ensure precise application in the form of narrow bands. A twin-trough chamber is used for chromatographic development, pre-saturated with the mobile phase for 20–30 minutes to achieve optimal separation. The mobile phase selected for eucalyptol is Toluene: Ethyl Acetate (9:1) in combination offers good resolution and efficient migration for non-polar terpenes. The development is carried out up to 70–80 mm from the base of the plate, and the spots are analysed under UV light at 540 nm after derivatization with anisaldehyde-sulfuric acid reagent.

Calibration curve Preparation

The calibration curve was plotted in the range of 92.25-1,107ng/spot, using data of peak areas against the corresponding amount per spot. This solution was used as a reference solution (stock solution) for eucalyptol.

Solubility Study

Screening of Oil

In the shake flask technique, several modified oils, surfactants, and co-surfactants have been proven to have transparency and rapid emulsification, and these qualities were employed in choosing the oils. Excess 1,8-Cineole was transferred to screw-capped vials and mixed (Vortex mixer, Remi, Mumbai, India) for 30s with 2mL of each excipient. The container was shaken for 72h at 120rpm in a water bath shaker at 37±0.5°C (Rivotek, Mumbai, India). After 72h, each container was centrifuged in a lab centrifuge (Remi Equipment, Mumbai, India) for 15min at 3000rpm. The supernatant was separated using membrane filtration and filter paper with a 0.45µm particle size. Methanol had been used to dilute the particular component. The total amount of the solubilized drug was determined using an established equation. The development is carried out up to 70–80 mm from the base of the plate, and the spots are analysed under UV light at 540 nm after derivatization with anisaldehyde-sulfuric acid reagent.

Screening of Surfactant and Co-Surfactant

Tween 80, Tween 20, Span 80, and Span 20 were selected as surfactants. Surfactants were mixed with the chosen oily phase at a 1:1 ratio (3 ml). To facilitate the homogenization of the components, the mixtures were heated to a comfortable 500°C. Each 0.5 mL combination was diluted with distilled water to 50 mL in a conical flask with a stopper. The number of flask inversions needed to achieve emulsification was determined. After 2 h, the development is carried out up to 70–80 mm from the base of the plate, and the spots are analysed under UV light at 540 nm after derivatization with anisaldehyde-sulfuric acid reagent. Additionally, turbidity and phase segregation in the emulsions were monitored.

Screening of Co-Surfactant

The PEG 400, PEG 200, and Propylene Glycol were selected as co-surfactants for the study. With 1 mL of co-surfactant and 2 mL of surfactants, the selected oily phase was diluted to a volume of 3 mL. The combinations were heated to 500°C to aid in the homogeneity of the components. Each 0.5 mL combination was diluted with water to 50 mL in a conical flask with a stopper. The number of times a flask had to be inverted before a homogeneous emulsion formed was used to measure how difficult it was to emulsify the mixture. After 2 h, the development is carried out up to 70–80 mm from the base of the plate, and the spots are analysed under UV light at 540 nm after derivatization with anisaldehyde-sulfuric acid reagent.

Determination of drug-polymer compatibility

FTIR Spectroscopy

The pure 1,8-Cineole and other excipients was taken liquid cells with appropriate window materials like **KBr**, an infrared transparent matrix at 1:100 (sample: KBr) ratio, respectively. The liquid cells were then scanned over a wave range of 4000 – 400 cm^{-1} and spectra was obtained by using a FTIR spectrometer-430 (Shimadzu 8400S, Japan).

Differential Scanning Calorimetry

Thermogram for drug and excipients separately and in blend was obtained using DSC (Mettler DSC 1 star system, Mettler-Toledo, Switzerland). The drug was sealed in perforated aluminum pan and heated at constant rate of 10°C/min over the temperature ranges of -10-350°C at 20ml/min nitrogen purging.

Construction of pseudo-ternary phase diagrams

The optimization of the 1,8-Cineole L-SNEDDS formulation involved constructing pseudo-ternary phase diagrams using TernaryPlot software at room temperature to define the concentration range suitable for L-SNEDDS. The water titration method was employed to identify regions capable of self-microemulsification upon dilution. Various combinations of surfactants and co-surfactants were tested, leading to pseudo-ternary phase diagrams that revealed the optimal formulations. The mixtures of oil, surfactant, and co-surfactant were prepared by diluting them in water and mixing with a magnetic stirrer, maintaining a total composition of 100%, with each component represented at a triangle vertex. To locate the self-microemulsion regions, several phase diagrams were plotted and compared based on the sizes of the emulsion zones through direct observation. Tween 80 and PEG-200 were combined in different weight ratios (Smix) such as 1:1, 1:2, and 2:1, while solubility studies supported the selection of 1,8-Cineole as the oil phase. Each diagram represented a specific combination of 1,8-Cineole and Smix ratios (e.g., 1:9, 2:8, 3:7, 4:6, etc.). The oil-to-Smix mixtures were titrated with water, blended using a magnetic stirrer, and visually analyzed to categorize the resulting solutions into distinct phases: transparent nanoemulsion (N.E.) with excellent flow, transparent microemulsion (M.E.) with medium flow, milky emulsion (E) with good flow, and milky gel emulgel (M) with good flow. In the diagrams, oil was denoted as point A, Smix as point B, and water as point C, with a separate phase diagram created for each Smix ratio. The nanoemulsion regions were shaded to distinguish them from other phases.

Formulation of L-SNEDDS (Ultrasonication)

Liquid self-nanoemulsifying drug delivery systems (L-SNEDDS) were developed using optimized proportions of 1,8-Cineole (X1 mL) as the lipid phase, Tween 80 (X2 mL) as the surfactant, and PEG-200 (X3 mL) as the co-surfactant. The components were precisely measured and transferred into a glass vial. The mixture was vortexed gently to obtain a preliminary uniform blend. To enhance the emulsification efficiency and achieve a finer droplet size, the pre-concentrate was subjected to ultrasonication using a probe ultra-sonicator (J.P Selecta, Barcelona, Spain) for 10 minutes. This step facilitated the reduction of oil droplet size and ensured better dispersion of the lipid phase in the surfactant system. Following sonication, the formulations were incubated in a water bath maintained at 37 ± 0.5 °C (Memmert GmbH & Co. KG, Schwabach, Germany) for 15 minutes, simulating physiological temperature conditions and promoting complete solubilization as given in Table 1 and 2.

Formulation Design

A RSM-CCD (Response Surface Methodology-Central Composite Design) design was constructed where the X_1, X_2 and X_3 were selected as the two independent variables. It is suitable for investigating the 2FI response surfaces and for constructing a second-order polynomial model, thus enabling optimization. The levels of the three factors were selected on the basis of the preliminary studies carried out before implementing the experimental design. All other formulation and processing variable were kept constant throughout the study. Optimization of L-SNEDDS done by Design expert 10 statistical software trial packages, Stat-Ease 10.0.3.1. All the above formulations were prepared and evaluated for various parameters. The data was inputted to design expert software and polynomial equation was obtained. The responses (dependent variables) studied were Y_1, Y_2.

A RSM-CCD design was chosen for the optimization of L-SNEDDS because it allows the determination of influence of the factors with a minimum number of experiments. The independent factors were amount of Oil (X_1), amount of Surfactant (X_2) and amount of Co-surfactant (X_3). The response variables were Droplet Size (nm) (Y_1) and Drug release (%CDR) (Y_2). 20 formulations were prepared according to factorial design. The formulations were F1 to F20. The responses obtained from the design matrix were statistically evaluated using Design expert 10 statistical software trial packages, Stat-Ease 10.0.3.1.

Optimization data analysis and model-validation

ANOVA was used to establish the statistical validation of the polynomial equations generated by Design Expert® Software (20–22). Fitting a multiple linear regression model to a RSM-CCD design give a predictor equation incorporating interactive and polynomial term to evaluate the responses:

$$Y = b0 + b1X1 + b2X2 + b3X3 + b12X1X2 + b23X2X3 + b13X1X3 + b11X1^2 + b22X2^2 + b33X3$$

----(1)

Where Y is the measured response associated with each factor level combination; b_0 is an intercept representing the arithmetic average of all quantitative outcomes of 20 runs; bi (b_1, b_2, b_3, b_{11}, b_{12}, b_{22} and b_{33} etc.) are regression coefficients computed from the observed experimental values of Y and X_1, X_2 and X_3 are the coded levels of independent variables. The terms X_1 X_2 and X_3 represent the interaction terms. Three-dimensional response surface plots resulting from equations were obtained by the Design Expert® software.

Table 1: Variables of CCD Design

Factor	Role	Low	High
1,8-Cineole (X_1 ml))	Oil	3 (-1)	6 (+1)
Tween 80 (X_2 ml)	Surfactant	2 (-1)	4 (-1)
PEG-200 (X_3 ml)	Co-surfactant	1 (-1)	2 (-1)

Table 2: Formulations Batches as per RSM-CCD design

Formulation Code	X_1 (ml)	X_2 (ml)	X_3 (ml)
F1	0	0	0
F2	0	1.68179	0
F3	1	-1	-1
F4	-1	1	1
F5	-1.68179	0	0
F6	1	1	-1
F7	-1	-1	1
F8	**1**	**1**	**1**
F9	0	0	0
F10	0	-1.68179	0
F11	1.68179	0	0
F12	0	0	-1.68179
F13	0	0	0
F14	0	0	0
F15	0	0	1.68179
F16	-1	-1	-1
F17	0	0	0
F18	1	-1	1
F19	0	0	0
F20	-1	1	-1

Characterization of L-SNEDDS

FTIR Spectroscopy

The L-SNEDDS was **taken liquid cells** with appropriate window materials like **KBr**, an infrared transparent matrix at 1:100 (sample: KBr) ratio, respectively. The liquid cells were then scanned over a wave range of 4000 – 400 cm^{-1} and spectra were obtained by using a FTIR spectrometer-430 (Shimadzu 8400S, Japan).

Differential Scanning Calorimetry

Thermogram for L-SNEDDS was obtained using DSC (Mettler DSC 1star system, Mettler-Toledo, Switzerland). The drug was sealed in perforated aluminum pan and heated at constant rate of 10°C/min over the temperature ranges of 30-350°C at 20ml/min nitrogen purging.

Measurement of Zeta potential and droplet size

The Malvern Instruments' Zetasizer, with its impeccable precision, was harnessed to ascertain the zeta potential of the L-SNEDDS droplets, offering insights into the electrostatic stability of the formulation. A specific ratio was maintained as 1 mL of the L-SNEDDS-F8 formulation was diluted with 100 mL of deionized water. To minimize scattering errors, transparent plastic cuvettes were used for

measurements. Furthermore, the system also facilitated the simultaneous determination of the droplet size, which is crucial for predicting the bio-distribution and intracellular uptake of the formulation.

Morphological characterization

A dual-pronged microscopic exploration, encompassing Scanning Electron Microscopy (SEM) and Transmission Electron Microscopy (TEM), was embarked upon. While SEM gives insights into surface topography, TEM allows for a profound understanding of internal microstructures. The rigorous sample preparation protocol, involving strategic staining and sectioning, assured unparalleled resolution and clarity.

Rheological study

The viscosity of the developing nanoemulsion was measured using a Brookfield viscometer (Brookfield Engineering Labs, St. Louis, MO, USA) with Small Sample Adapter beginning at 20rpm at 25°C after the BD-loaded optimized L-SNEDDS formulation was diluted with water in a ratio of 1:250.

Determination of Refractive Index

The refractive index of the L-SNEDDS formulation was determined using an Abbe refractometer at room temperature (25°C). The instrument was first calibrated using distilled water, which has a known refractive index of 1.3330. A few drops of the L-SNEDDS were placed on the prism, ensuring no air bubbles were trapped, and the refractive index was recorded. The measurement was performed in triplicate, and the mean ± standard deviation was calculated. A refractive index value close to that of water indicates isotropy and optical clarity of the nanoemulsion, confirming the uniform dispersion of nano-sized droplets.

***In-Vitro* Release Study**

The *in-vitro* drug release study for 1,8-Cineole-loaded L-SNEDDS formulations was performed using USP Dissolution Test Apparatus-II (paddle method) from Electrolab, USA. The dissolution medium consisted of 900 mL of PBS 7.4, maintained at 37±0.5°C to simulate physiological conditions. The paddle rotation speed was set at 50 rpm. At predetermined time intervals (5, 10, 15, 20, 25, 30, 45, and 60 minutes), 5 mL aliquots of the dissolution medium were withdrawn for analysis. To maintain a constant volume, an equal amount of fresh dissolution medium was replenished after each sampling. The withdrawn samples were filtered through a 0.45µm Whattman filter paper (Whattman, NJ, USA) to remove un-dissolved particles. The filtrates were then analyzed for drug content using a validated analytical technique, such as HPTLC (the spots are analysed under UV light at 540 nm after derivatization with anisaldehyde-sulfuric acid reagent), to determine the concentration of the released drug.

Stability Study of L-SNEDDS

The thermodynamic stability of the optimized L-SNEDDS formulation was evaluated through a series of stability tests to ensure its robustness and suitability for long-term use.

Heating-Cooling Cycle: The formulation was subjected to six consecutive cycles of temperature variation between 4°C and 45°C, with each temperature maintained for at least 48 hours. This test was conducted to assess the formulation's ability to withstand thermal stress without showing signs of instability, such as creaming or cracking.

Centrifugation Test: Formulations that passed the heating-cooling cycle were further subjected to centrifugation at 3,500 rpm for 30 minutes. This test was designed to evaluate the physical stability of the formulation under stress conditions, such as phase separation or precipitation.

Only formulations that exhibited no signs of instability during both tests were considered thermodynamically stable, indicating their potential for maintaining physical integrity during storage and transportation.

Solidifications of L-SNEDDS and Filing in the Capsules

Lyophilization, or freeze-drying, is a process that removes water from a product after freezing and placing it under a vacuum, allowing the ice to change directly from solid to vapor without passing through a liquid phase. In the lyophilization of L-SNEDDS, the process begins with preparing a homogeneous solution by dissolving the liquid SNEDDS formulation with a suitable carrier (e.g., mannitol) in a common solvent. The solution is then frozen at temperatures between −50°C and −80°C to ensure the formation of solid ice crystals. During primary drying (sublimation), reduced pressure and controlled heat supply allow ice to sublimate, removing about 95% of the water content. This is followed by secondary drying (desorption), where a higher temperature eliminates any residual unfrozen water, reducing the final moisture content to 1–4%. This process effectively converts L-SNEDDS into a solid form while maintaining its self-emulsifying properties, facilitating further processing into solid dosage forms like capsules as shown in Table 12.

Flow properties

Flow properties such as angle of repose, bulk density, tapped density and compressibility index of optimized formulations, and were evaluated to determine the suitability for capsule formulation

Angle of repose

Angle of repose was determined by using fixed funnel method. The powders were allowed to flow through the funnel fixed on a burette stand at definite height (h). The angle of repose (θ) was then calculated by measuring the height (h) and radius(r) of the heap of powder formed. Tan θ = h/r or θ = tan-1(h/r) ------- (4)

Bulk density

The bulk density of powder is dependent on particle packing and changes as powder consolidates. Apparent bulk density was determined by pouring a weighed quantity of powder into a graduated cylinder and measuring the volume of packing.

Bulk density = Weight of the powder / Volume of the packing ----- (5)

Tapped density

Tapped density is defined as the mass of a powder divided by the tapped volume. Tapped density was determined by tapping method. Weighed quantity of powder was placed in a graduated cylinder and tapped until no further change in volume of powder was noted and the volume of tapped packing was noted.

Tapped density = weight of the powder / volume of the tapped packing ------ (6)

Carr's index

The compressibility of the powder was calculated by determining the Carr's index.

Carr's Index = Tapped Density-Bulk density/Tapped density X 100 ------- (7)

Hausner's ratio

The Hausner's ratio of the powder was calculated by determining the Carr's index.

Hausner's ratio = Tapped density/Bulk density ------- (8)

Uniformity of weight

Intact capsule was weighed. The capsules were opened without losing any part of the shell and contents were removed as completely as possible. The shell was washed with ether and the shell allowed to stand until the odor of the solvent was no longer detectable. The empty shell was weighed. The average weight was determined. Not more than two of the individual weights deviate from the average weight by more than the percentage deviation and none deviates by more than twice that percentage.

Drug content

Five capsules were selected randomly and the average weight was calculated. An amount of powder was equivalent to 276 mg of 1,8-Cineole was made upto 100 ml with phosphate buffer pH 7.4. It was kept overnight. 1 ml of solution was diluted to 50 ml using phosphate buffer pH 7.4 in separate standard flask. The filtrates were then analyzed for drug content using a validated analytical technique, such as HPTLC (the spots are analysed under UV light at 540 nm after derivatization with anisaldehyde-sulfuric acid reagent), to determine the concentration of the released drug.

***In-Vitro* Release Study**

The *in-vitro* drug release study for 1,8-Cineole-loaded S-SNEDDS formulations was performed using USP Dissolution Test Apparatus-II (paddle method) from Electrolab, USA. The dissolution medium consisted of 900 mL of PBS 7.4, maintained at 37±0.5°C to simulate physiological conditions. The paddle rotation speed was set at 50 rpm. At predetermined time intervals (5, 10, 15, 20, 25, 30, 45, and 60 minutes), 5 mL aliquots of the dissolution medium were withdrawn for analysis. To maintain a constant volume, an equal amount of fresh dissolution medium was replenished after each sampling. The withdrawn samples were filtered through a 0.45µm Whattman filter paper (Whattman, NJ, USA) to remove un-dissolved particles. The filtrates were then analyzed for drug content using a validated analytical technique, such as HPTLC (the spots are analysed under UV light at 540 nm after derivatization with anisaldehyde-sulfuric acid reagent), to determine the concentration of the released drug.

Stability studies

The stability of capsule was monitored up to 90 days at ambient temperature and relative humidity (40°C/75%RH). Periodically samples were withdrawn and characterized by Physical Appearance, Drug Content and Dissolution.

RESULT AND DISCUSSION

Preformulation study

Identification and Confirmation of Drug

Identification and Confirmation of drug was carried out by boiling point method, DSC, FTIR and HPTLC.

Boiling Point Method

The observed boiling point of 1,8-Cineole was confirmed as shown in Table 3.

Table 3: Boiling Point of 1,8-Cineole

Sr. No.	Method	Observed Boiling Point
1.	Boiling Point Method	176-177°C

FTIR Analysis

In Figure 1, the FTIR spectrum of 1,8-cineole (eucalyptol) shows characteristic peaks at 2850–2960 cm^{-1} for aliphatic C-H stretching, 1050–1150 cm^{-1} for C-O-C stretching of the cyclic ether, 1350–1450 cm^{-1} for aliphatic C-H bending, and 700–900 cm^{-1} for out-of-plane cyclic C-H bending. The fingerprint region (600–1500 cm^{-1}) displays drug vibrations unique to its structure, while the absence of peaks at 3200–3600 cm^{-1} confirms no O-H or N-H groups are present. These features align with the molecular structure of 1,8-cineole.

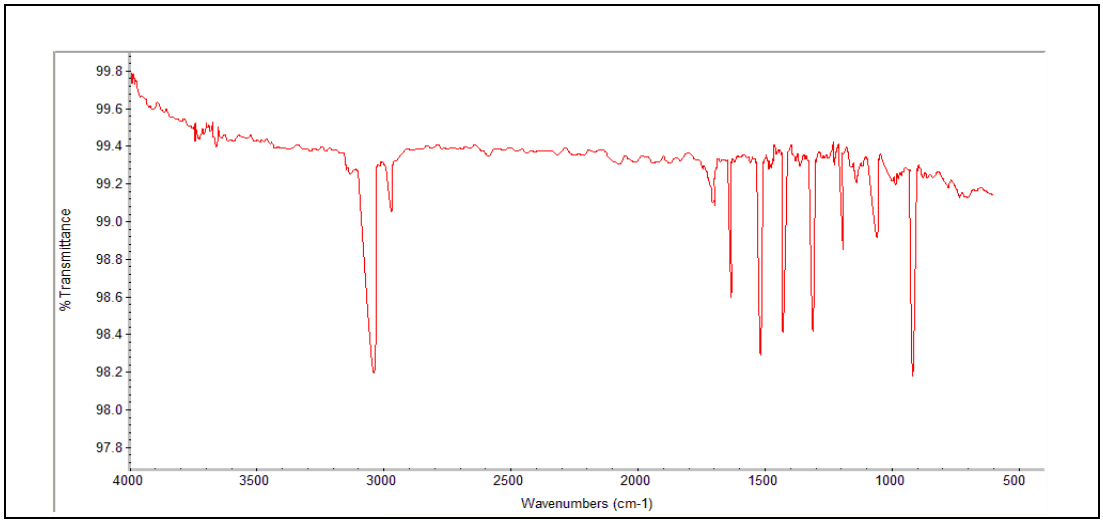

Figure 1: FTIR spectra of 1,8-Cineole

Differential Scanning Calorimetry

The Differential Scanning Calorimetry (DSC) analysis of the 1,8-Cineole, conducted at a scanning rate of 10°C/min, displayed no endothermic peak as illustrated in Figure 2. The melting point of 1,8-cineole is approximately 1.5°C (reported: https://pubchem.ncbi.nlm.nih.gov/compound/2758).

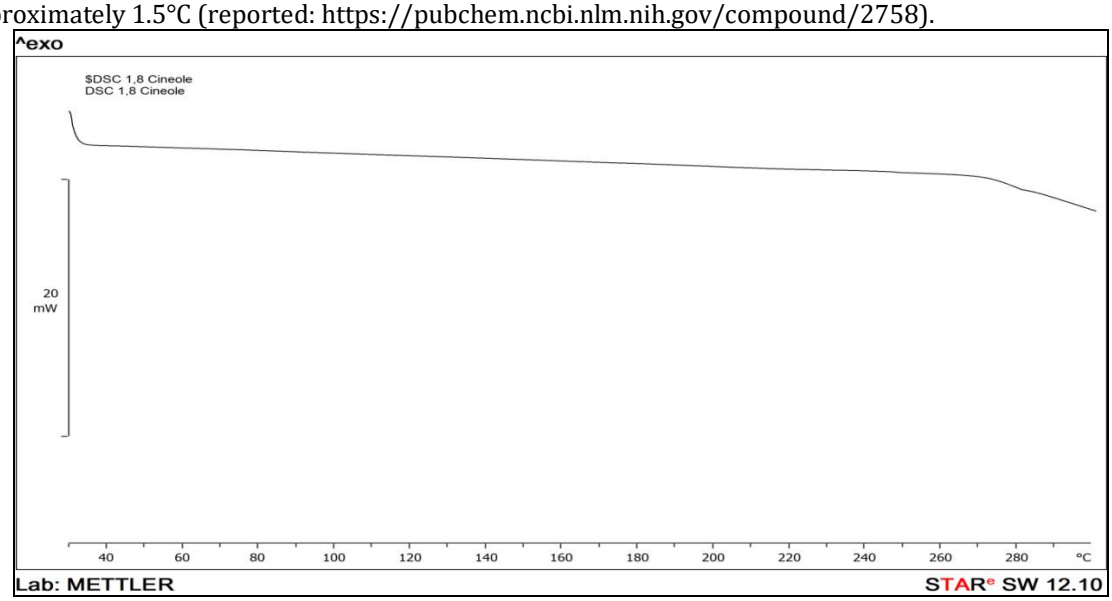

Figure 2: DSC spectra of 1,8-Cineole

Calibration curve Preparation

The calibration curve was plotted in the range of 92.25-1,107 ng/spot, using data of peak areas against the corresponding amount per spot. This solution was used as a reference solution (stock solution) for eucalyptol as shown in Table 4.

Table 4: Calibration Curve

Concentration (ng/spot)	Absorbance (AU)
92.25	6113.92
184.50	6999.87
369.00	8763.35
553.50	10526.83
738.00	12290.31
922.50	14053.78
1107.00	15817.26

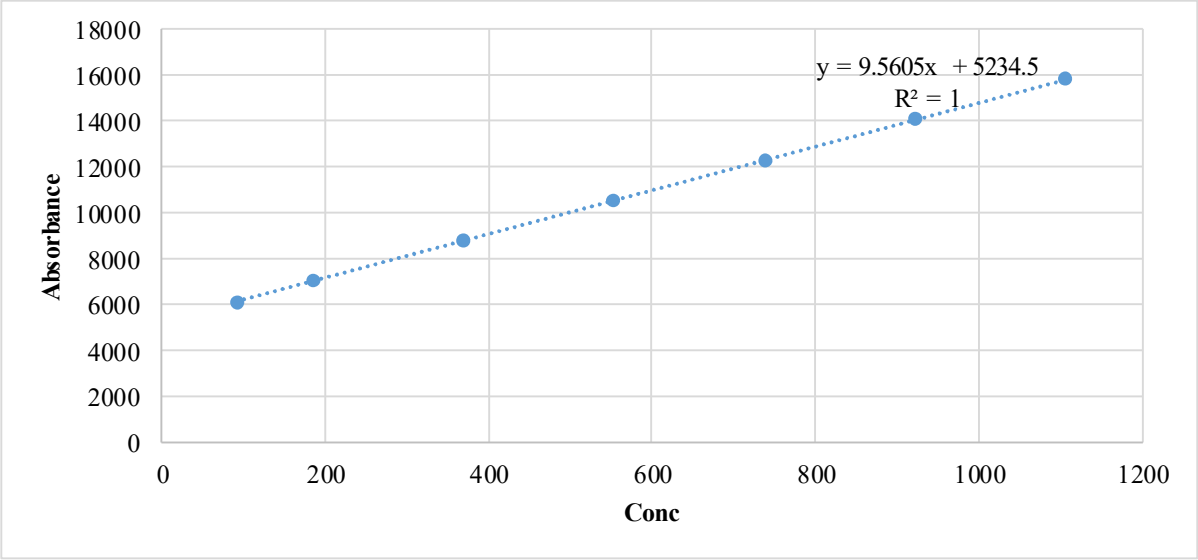

Figure 2 (A): Calibration curve of 1,8-Cineole

The mobile phase composed of Toluene: Ethyl Acetate (9:1) resulted in a sharp, symmetrical, and well-resolved peak at Rf values of 0.56 ± 0.04 for 1,8-Cineole, respectively.

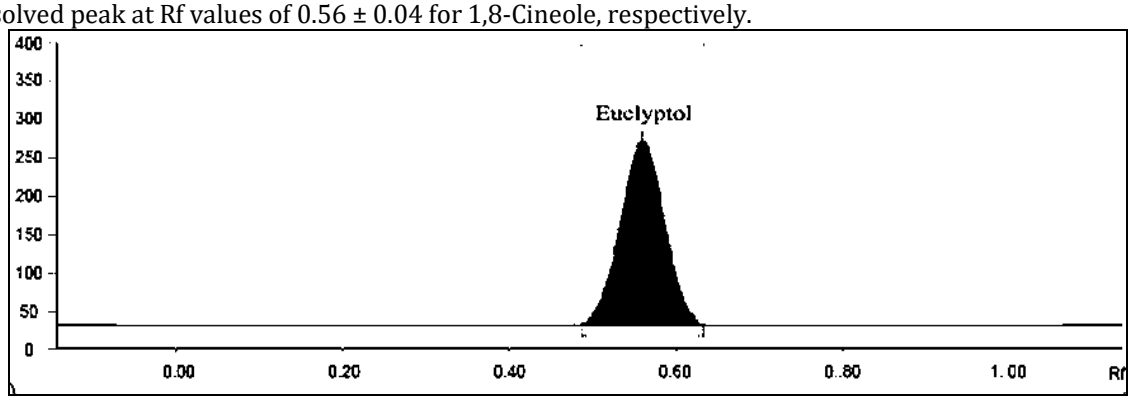

Figure 2 (B): Chromatograms of 1,8-Cineole standard

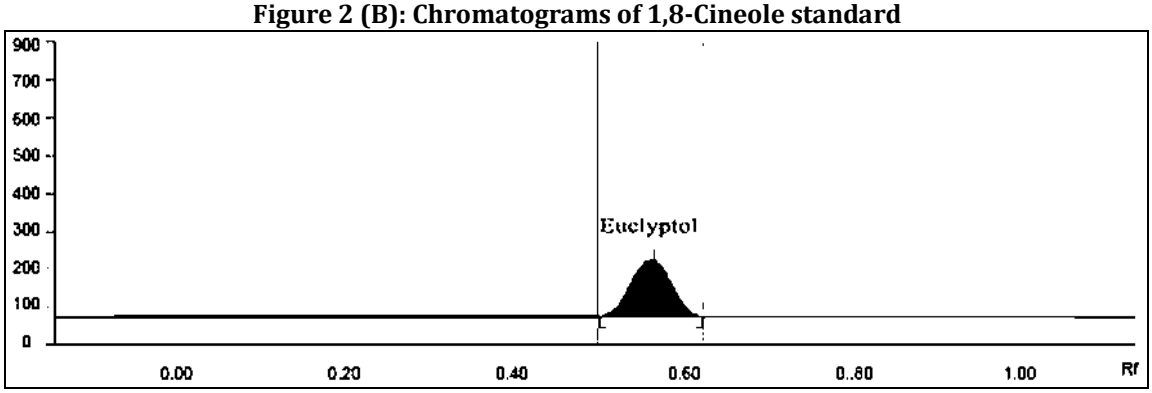

Figure 2 (C): Chromatogram of 1,8-Cineole in formulation (F8)

Comprehensive screening of oils, surfactants, and co-surfactants for optimal solubility

A solubility study was performed to find the best oil, surfactant, and co-surfactant to use in the formulation of 1,8-Cineole SNEDDS. 1,8-Cineole was chosen as the oil phase. Similarly, Table 5 demonstrates that Tween 80 has a maximum solubility as a 738.00 ng/spot surfactant. Table 5 displays the solubility of 1,8-Cineole in the cosurfactant PEG 200 (621.15 ng/spot). The solubility study aimed to locate appropriate SNEDDS components with a high capacity for 1,8-Cineole solubilization. 1,8-Cineole, Tween 80, and PEG200 were shown to have the highest solubilizing capability compared to the other oils, surfactants, and co-surfactants evaluated. Components of 1,8-Cineole SNEDDS include 1,8-Cineole, Tween 80, and PEG200. This decision was reached based on the solubility study.

Table 5: Screening Study

Sr. No.	Oil/Surfactant/Co-Surfactant	Reported Solubility (ng/spot)
1.	**1,8-Cineole (Oil)**	**184.50 (Methanol)**
2.	**Surfactant: Tween 80**	**738.00**
	Tween 20	542.24
	Span 80	445.20
	Span 20	418.21
3.	Co-Surfactant: PEG 400	338.28
	PEG 200	**621.15**
	Propylene Glycol	238.22

Tween 80 was used as a surfactant, achieving an entrapment efficiency of 77.49%. While these studies indicate that Tween 80 and PEG 200 can effectively solubilize 1,8-cineole, precise solubility values are not specified. Therefore, empirical testing is recommended to determine the exact solubility of 1,8-cineole in these excipients under specific conditions.

Drug-Excipients Compatibility Study

FTIR Analysis

In Figure 1, 3-6 the FTIR spectra are depicting the 1,8-Cineole and the physical mixture comprising all excipients (Oil, Tween 80 and PEG200). The FTIR spectra exhibit characteristic peaks at 2850–2960 cm^{-1} for aliphatic C-H stretching, 1050–1150 cm^{-1} for C-O-C stretching of the cyclic ether, 1350–1450 cm^{-1} for aliphatic C-H bending, and 700–900 cm^{-1} for out-of-plane cyclic C-H bending. The fingerprint region (600–1500 cm^{-1}) displays drug vibrations unique to its structure, while the absence of peaks at 3200–3600 cm^{-1} confirms no O-H or N-H groups are present, respectively. Notably, all these peaks remain unchanged, showing no significant alterations in the characteristic peaks of the pure drug when compared to the physical mixture. This suggests that the drug is compatible with the other excipients.

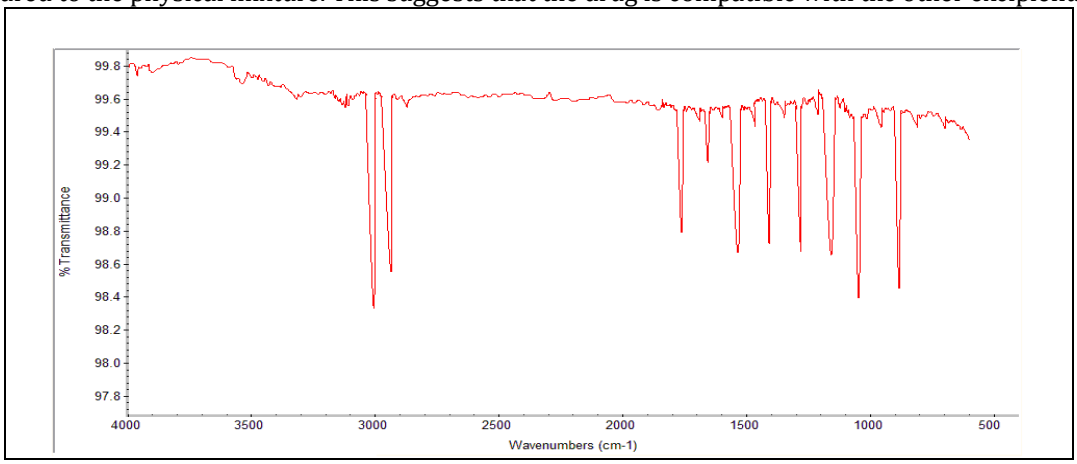

Figure 3: FTIR spectra of 1,8-Cineole

The FTIR spectrum of pure 1,8-Cineole exhibits key characteristic peaks that confirm its functional groups. The strong absorption around 2965–2850 cm^{-1} corresponds to C–H stretching of methyl and methylene groups, while a prominent peak near 1050–1070 cm^{-1} is attributed to the C–O–C asymmetric stretching of the ether group.

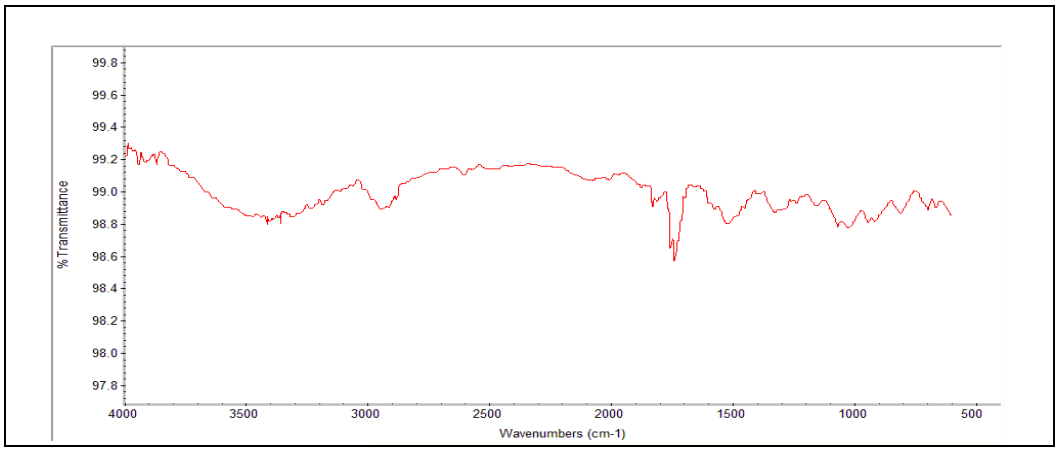

Figure 4: FTIR spectra of Tween 80

Tween 80 shows characteristic bands around 1735 cm^{-1} (C=O stretching of ester), 2880–2950 cm^{-1} (C–H stretching), and a broad band in the 3400–3500 cm^{-1} range due to O–H stretching. These peaks do not overlap or interfere with the characteristic ether band of 1,8-Cineole at ~1050 cm^{-1}. In the physical mixture, the retention of 1,8-Cineole's key peaks suggests that Tween 80 does not interact chemically with the drug, indicating compatibility.

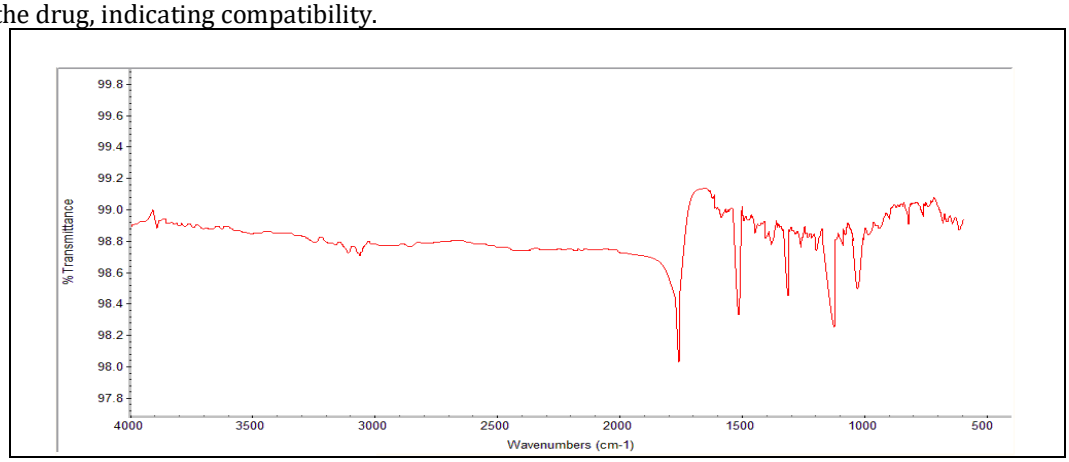

Figure 5: FTIR spectra of PEG 200

PEG 200 displays a strong and broad O–H stretching band around 3400 cm^{-1}, along with C–H stretching at ~2880–2940 cm^{-1}, and a C–O–C stretching band near 1100 cm^{-1}. While there may be some overlap in the C–O–C region with 1,8-Cineole, the characteristic ether peak of the drug remains visible in the physical mixture. No new peaks or significant shifts are observed, suggesting no interaction between PEG 200 and 1,8-Cineole.

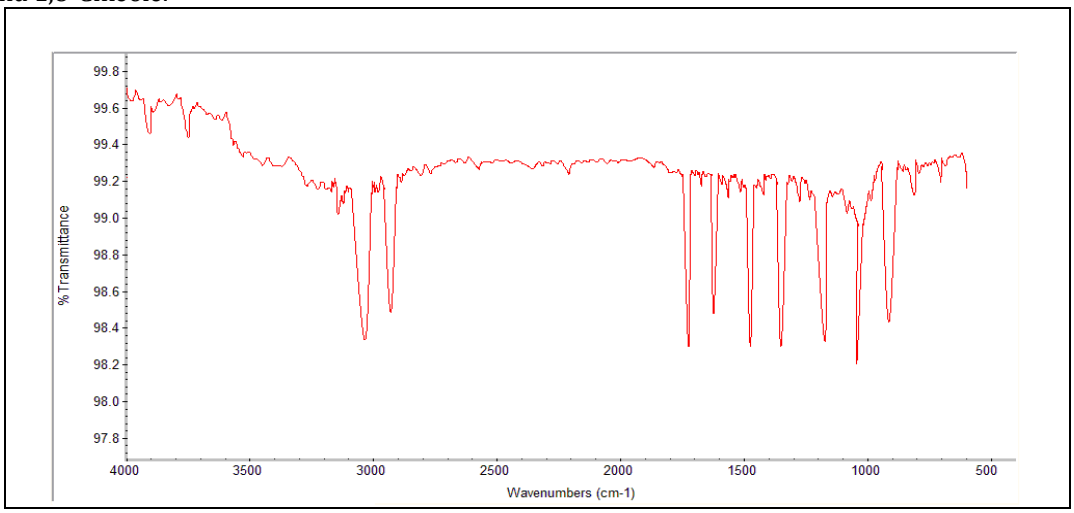

Figure 6: FTIR spectra of Physical Mixture

The spectrum of the physical mixture clearly retains the major peaks of 1,8-Cineole (~2960, 2850, and 1050 cm^{-1}) along with identifiable bands from both Tween 80 and PEG 200. There is no disappearance or significant shift of characteristic peaks, and no new bands appear. This supports the conclusion that no significant chemical interactions have occurred among the components, confirming the compatibility of 1,8-Cineole with both Tween 80 and PEG 200 in the SNEDDS formulation.

Differential Scanning Calorimetry

Differential Scanning Calorimetry (DSC) has been proposed as a rapid technique to evaluate the physical and chemical interactions within a formulation. It involves comparing the thermal profiles of pure substances with a 1:1 physical mixture, aiding in the identification of suitable excipients for compatibility. In this context, analysis of the DSC thermograms revealed a distinctive melting point for the drug at 1.5°C (reported: https://pubs.acs.org/doi/10.1021/jp067405b). The DSC thermograms of Tween 80 and PEG 200 displayed melting points at 111.38°C and 73.83°C, respectively, and when combined with the oil, no discernible shifts in these peaks were observed. This absence of shift indicates compatibility between the drug and both Tween 80 and PEG 200. Figures 2, 7-10 illustrate the comparison of DSC thermograms for the 1,8-Cineole, individual excipients, and drug-excipient mixtures.

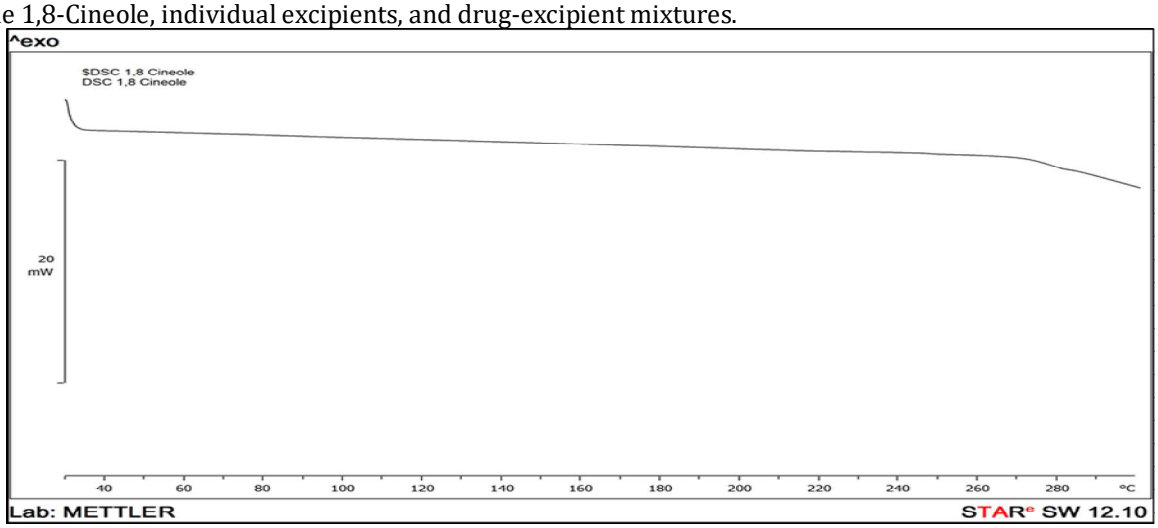

Figure 7: DSC spectra of 1,8-Cineole

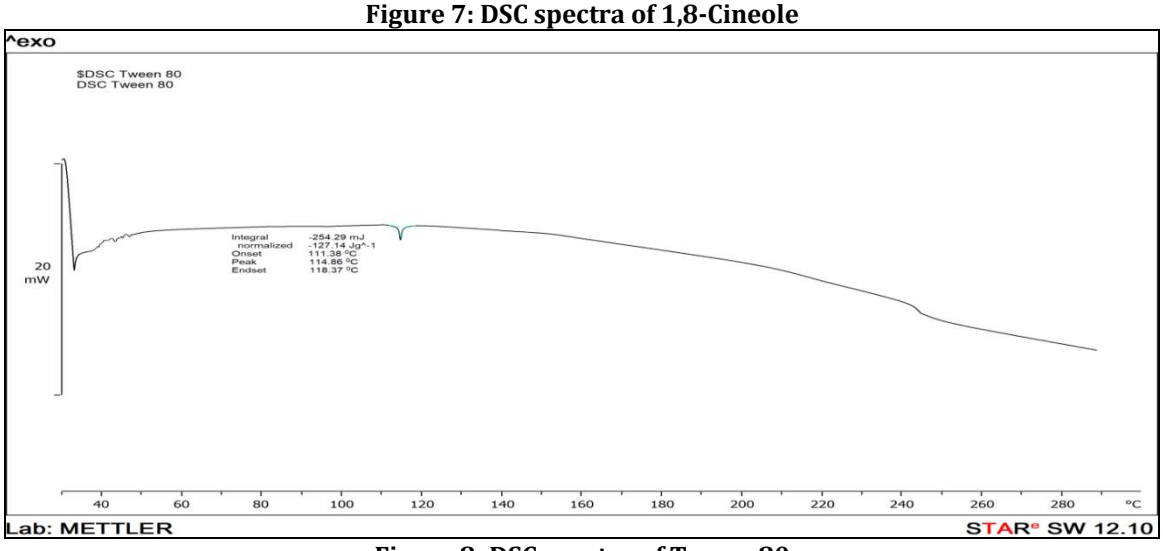

Figure 8: DSC spectra of Tween 80

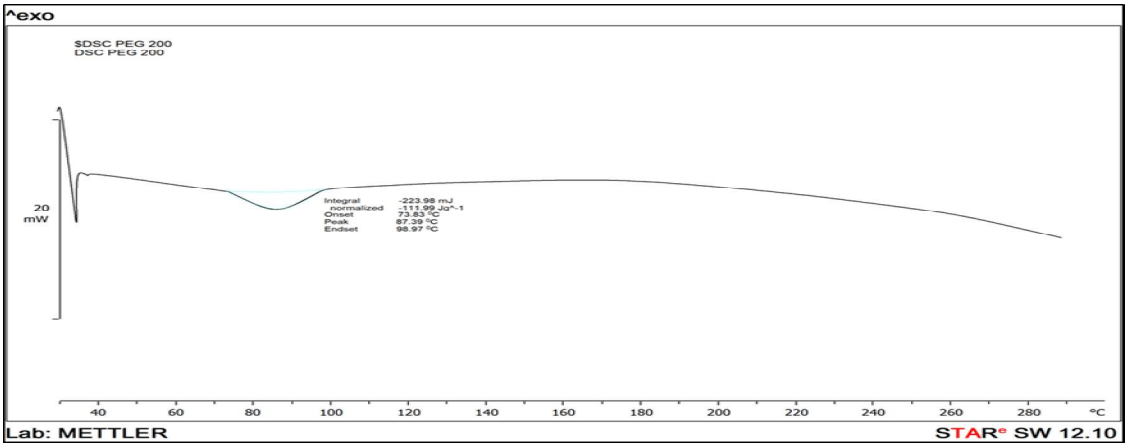

Figure 9: DSC spectra of PEG 200

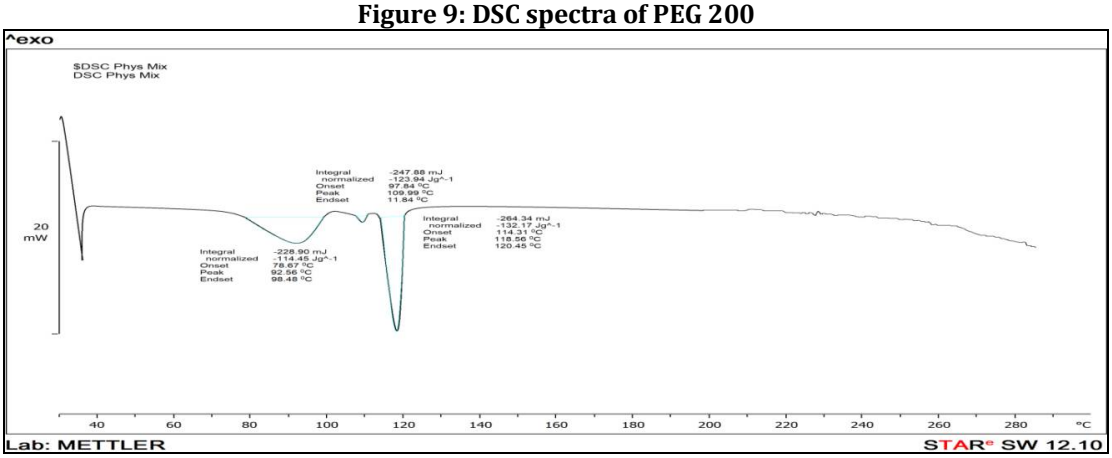

Figure 10: DSC spectra of Physical Mixture

Construction of pseudo-ternary phase diagrams

The phase diagram with a 2:1 Smix ratio showed the broadest emulsification region, making it ideal for developing the 1,8-Cineole L-SNEDDS. 1,8-Cineole (5–50%), Tween 80 (20–60%), and PEG 200 (10–25%) were selected as the oil, surfactant, and co-surfactant, respectively, based on optimal nanoemulsion stability and drug release performance.

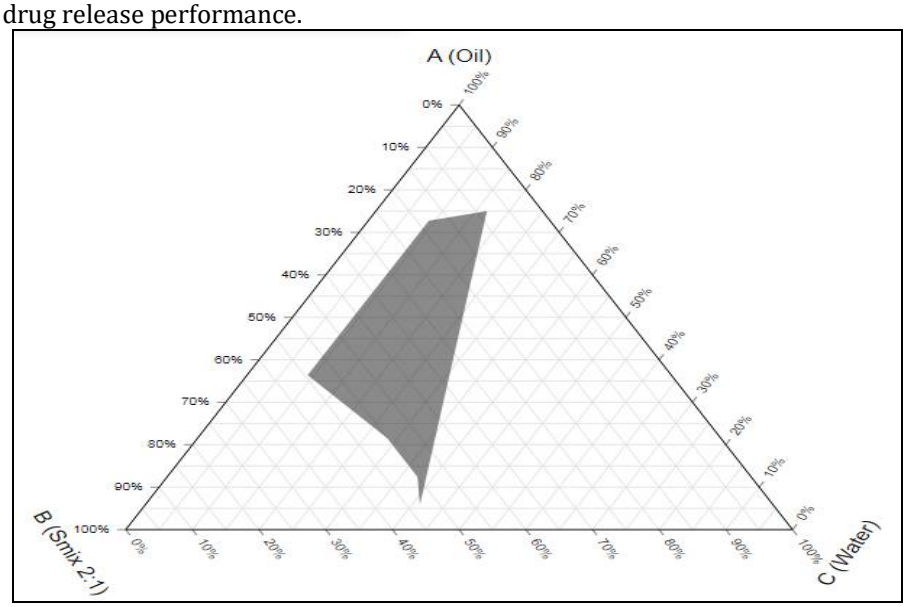

Figure 11: The phase diagram with a 2:1 Smix ratio

Formulation Design

The RSM central composite designs (CCD) with results are shown in Tables 6. All the batches were formulated and evaluated for droplet size and %CDR. The obtained results provided considerable useful information and confirmed the utility of the statistical design for the conduction of the experiments.

Independent variables such as oil amount (X_1ml), the amount of surfactant (X_2ml), and amount of co-surfactant (X_3ml) significantly influenced the observed responses, droplet size (Y_1 d.nm), and %CDR (Y_2 %). The optimized formulation batch was determined by systematic analysis of data using design expert software.

Table 6: Design Batches

Formulation Code	X_1(ml)	X_2(ml)	X_3(ml)	Y1 (d.nm)	Y2 (%)
F1	4.5	3	1.5	115	81.36
F2	4.5	4.68179	1.5	175	79.56
F3	6	2	1	114	81.64
F4	3	4	2	124	75.47
F5	1.97731	3	1.5	165	71.98
F6	6	4	1	135	73.56
F7	3	2	2	125	70.69
F8	**6**	**4**	**2**	**110**	**89.90**
F9	4.5	3	1.5	130	71.72
F10	4.5	1.31821	1.5	145	81.83
F11	7.02269	3	1.5	225	81.11
F12	4.5	3	0.659104	243	80.79
F13	4.5	3	1.5	220	79.78
F14	4.5	3	1.5	190	78.65
F15	4.5	3	2.3409	215	87.45
F16	3	2	1	198	81.41
F17	4.5	3	1.5	220	82.45
F18	6	2	2	210	83.14
F19	4.5	3	1.5	225	82.44
F20	3	4	1	385	80.45

Optimization data analysis and model-validation:

A) Fitting of data to model:

The three factors with lower and upper design points in coded and un-coded values are shown in table 5. The ranges of responses Y_1 and Y_2 were 110-385 d.nm and 70.69-89.64% respectively. All the responses observed for nine formulations prepared were fitted to 2FI model, which was found as the best fitted model for Y_1 and Y_2, using Design Expert® software. The values of R^2, adjusted R^2, predicted R^2, SD and % CV are given in (Table 7), along with the regression equation generated for each response. The results of ANNOVA in (Table 8 and 9), for the dependent variables demonstrate that the model was significant for all the response variables. It was observed that independent variables X_1 (ml), X_2 (ml) and X_3 (ml) had a positive effect on the %CDR and a desired droplet size of nano-formulation i.e. L-SNEDDS was achieved.

Table 7: Summary of results of regression analysis for responses Y1 and Y2

Models	R^2	Adjusted R^2	Predicted R^2	SD	%CV
Response (Y1) 2FI	0.6404	0.4744	0.0385	47.39	25.83
Response (Y2) 2FI	0.6408	0.4751	0.2761	3.58	4.49

Regression Equations:

$Y1 = +183.45 - 11.87^{*}A + 11.53^{*}B - 22.71^{*}C - 33.13^{*}AB + 50.63^{*}AC - 38.63^{*}BC$ ---------- (9)

$Y2 = +79.76 + 2.59^{*}A - 0.1155^{*}B + 0.9578^{*}C - 0.6750^{*}AB + 4.16^{*}AC + 2.54^{*}BC$ ---------- (9)

B) Model Assessment for Dependent Variables:

After putting the data in Design Expert® software for, fit summary applied to data in that 2FI Model had been suggested by the software for all the responses. The statistical evaluation was performed by using ANNOVA. Results are shown in (Table 8 and 9). The coefficients with more than one factor term in the regression equation represent interaction terms. It also shows that the relationship between factors and responses is not always linear. When more than one factor are changes simultaneously and used at different levels in a formulation, a factor can produce different degrees of responses.

Table 8: Results of Analysis of Variance for Measured Response Y1

Source	Sum of Squares	df	Mean Square	F-value	p-value	
Model	51996.43	6	8666.07	3.86	0.0197	significant
A-Oil	1923.87	1	1923.87	0.8565	0.3716	
B-Surfactant	1815.33	1	1815.33	0.8082	0.3850	
C-Co-Surfactant	7040.86	1	7040.86	3.13	0.1001	
AB	8778.13	1	8778.13	3.91	0.0697	
AC	20503.13	1	20503.13	9.13	0.0098	
BC	11935.13	1	11935.13	5.31	0.0383	
Residual	29200.52	13	2246.19			
Lack of Fit	17217.19	8	2152.15	0.8980	0.5761	not significant
Pure Error	11983.33	5	2396.67			
Cor Total	81196.95	19				

Table 9: Results of Analysis of Variance for Measured Response Y2

Source	Sum of Squares	df	Mean Square	F-value	p-value	
Model	297.73	6	49.62	3.87	0.0195	significant
A-Oil	91.32	1	91.32	7.11	0.0194	
B-Surfactant	0.1823	1	0.1823	0.0142	0.9070	
C-Co-Surfactant	12.53	1	12.53	0.9760	0.3412	
AB	3.64	1	3.64	0.2840	0.6031	
AC	138.44	1	138.44	10.79	0.0059	
BC	51.61	1	51.61	4.02	0.0662	
Residual	166.87	13	12.84			
Lack of Fit	84.80	8	10.60	0.6457	0.7229	not significant
Pure Error	82.08	5	16.42			
Cor Total	464.61	19				

C) 3D Surface Plot Analysis

The 3D surface data reveals significant interactions between the independent variables (X_1, X_2 and X_3) and their impact on droplet size (Y_1) and %CDR (Y_2). Notably, F8, with X_1= 6; X_2=4; X_3=2, achieves the smallest particle size (Y_1=110nm) and highest %CDR (Y_2=89.64%), suggesting synergistic interactions. Variability among formulations with similar X_1, X_2, and X3 values, such as F1, F13, and F17, indicates the influence of experimental conditions and emphasizes the importance of further optimization through detailed 3D analysis as shown in **Figures 12A-12D.**

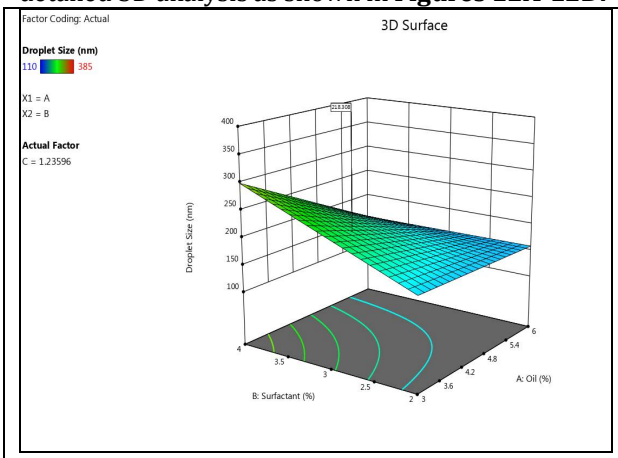

(A)

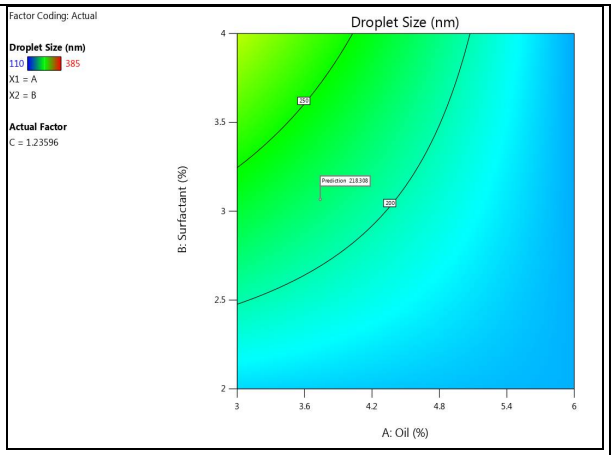

(B)

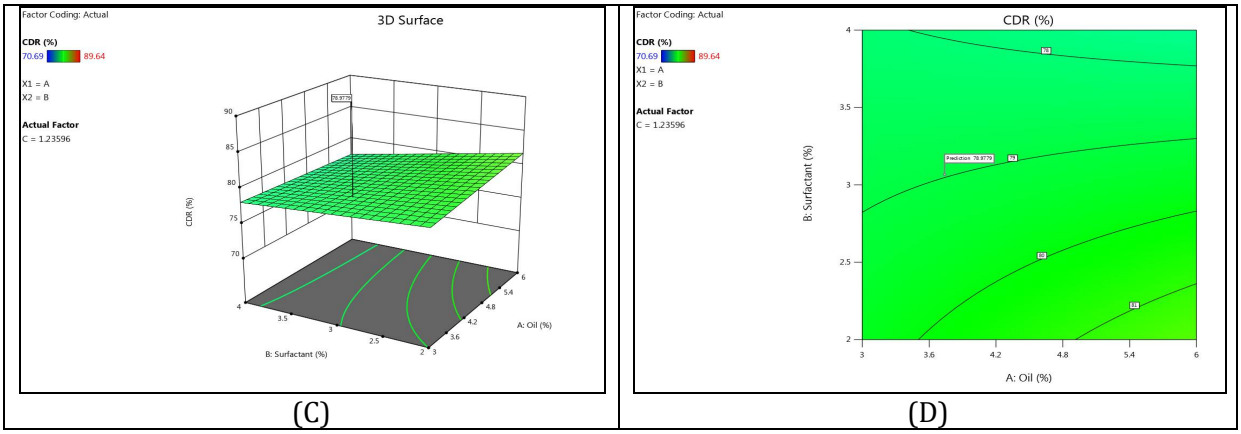

Figure 12: A) 3D surface plots Droplet Size (Y1); B) Contour plot of droplet Size; C) 3D surface plots on %CDR (Y2); D) Contour plot of %CDR

Characterization of L-SNEDDS

FTIR Spectroscopy

The FTIR spectra of L-SNEDDS of F8 are shown in Figure 16. The L-SNEDDS of F8 showed the characteristic peaks of both drug and excipients, showing that the drug was still present in the mixture and had not experienced any molecular changes or interactions with carriers (Tween 80 & PEG200).

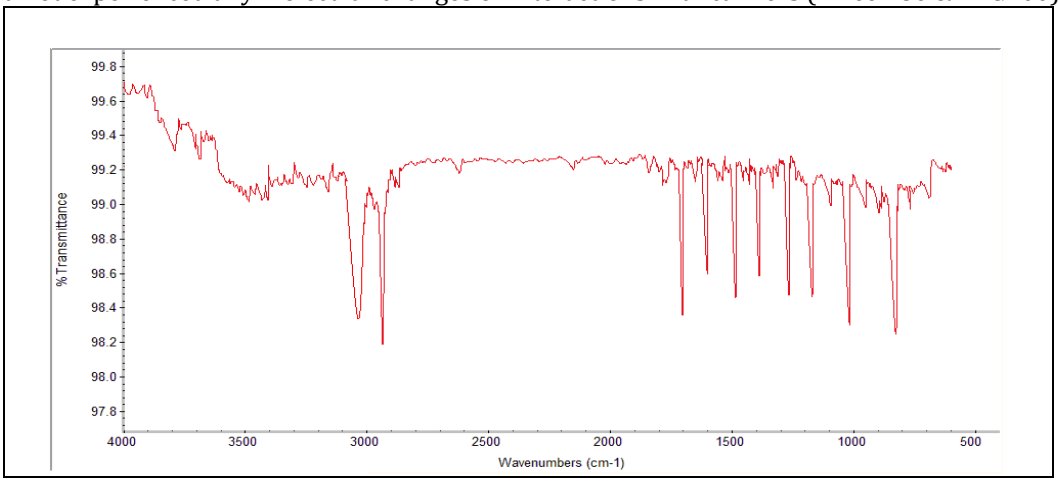

Figure 13: FTIR spectra of F8 Formulation

Differential Scanning Calorimetry

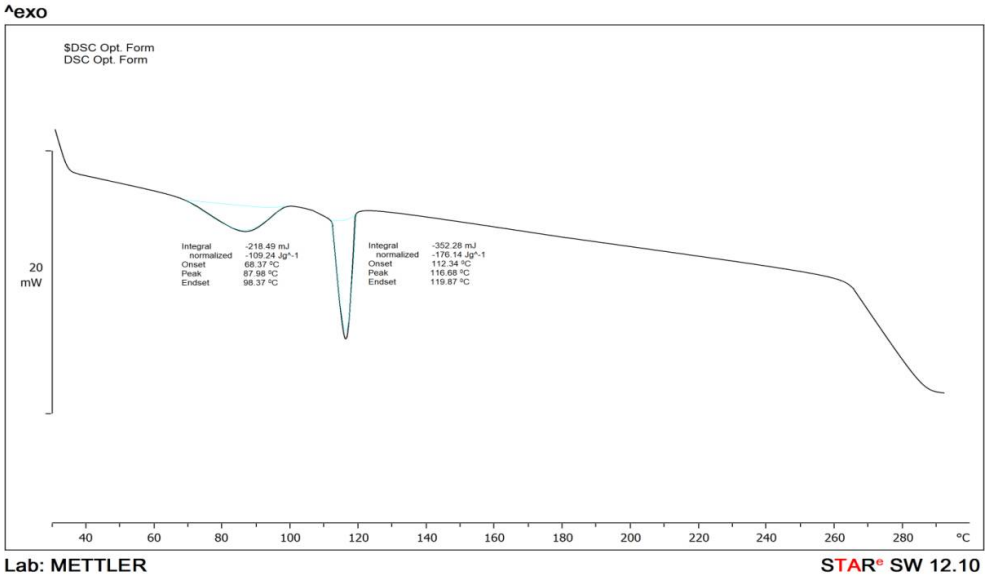

Figure 14: FTIR spectra of F8 Formulation

The Differential Scanning Calorimetry (DSC) analysis of the F8 formulation revealed no significant shifts or changes in the melting points of 1,8-Cineole, Tween 80, and PEG 200, indicating good compatibility between the drug and the excipients. The melting point of 1,8-Cineole was observed at 1.5°C (https://pubchem.ncbi.nlm.nih.gov/compound/2758), while Tween 80 and PEG 200 displayed melting points at 111.38°C and 73.83°C, respectively as shown in Figure 17, with no alteration when combined in the formulation. This absence of peak shifts or the appearance of new peaks suggests that there are no significant physical or chemical interactions between the drug and excipients, implying that the F8 formulation is thermodynamically stable. These findings support the suitability of this formulation for 1,8-Cineole delivery systems, ensuring that the drug's stability, release, and efficacy are not compromised by the excipient-drug interactions.

Measurement of Zeta potential and droplet size

The zeta potential is an important indicator of formulation stability, as it predicts the potential for particle aggregation. A higher absolute value of zeta potential indicates stronger repulsive forces between particles, decreasing aggregation chances. A negative zeta potential usually signals a stable colloidal system. In the case of L-SNEDDS F8, a zeta potential of -17.54 mV (Figure 16) reflects good physical stability and suggests the presence of negatively charged entities on the droplet surface, likely due to free fatty acids in the oil phase. Regarding droplet dynamics, the mean diameter of the dispersed phase for F8 was found to be 110.3 nm (Figure 15), with a Polydispersibility Index (PDI) of 0.049. A low PDI value indicates a uniform size distribution, which is favorable for consistent drug release and overall formulation stability.

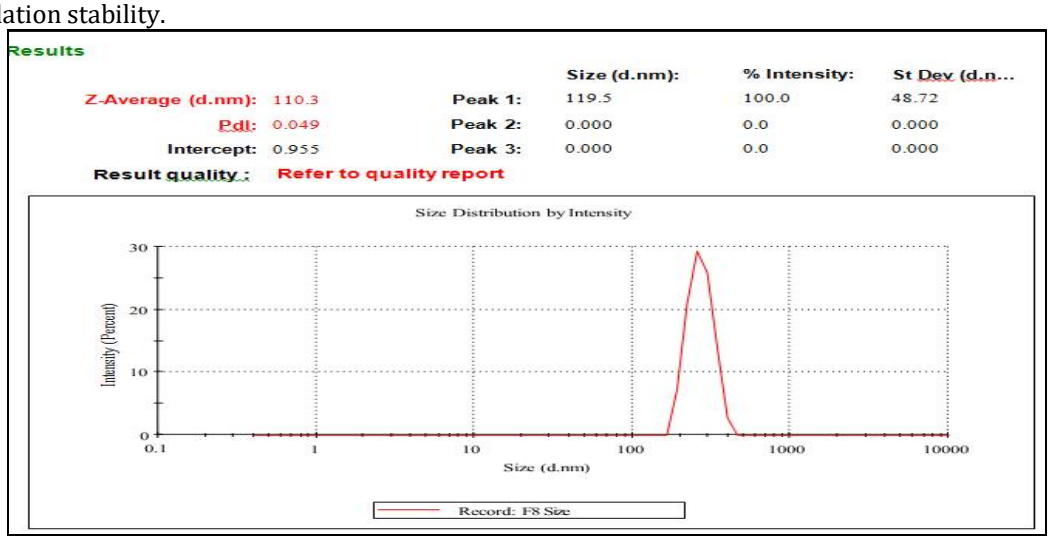

Figure 15: Particle Size of F8 Formulation

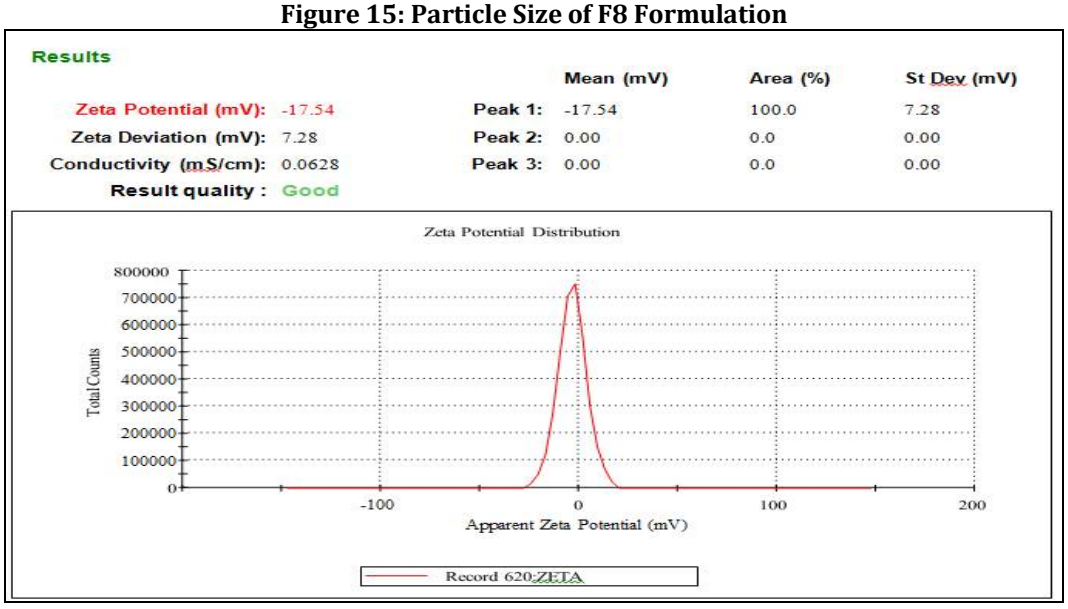

Figure 16: Zeta Potential of F8 Formulation

Morphological Characterization

SEM

Morphological examination through scanning electron microscopy (SEM) is crucial for understanding the shape, size, and uniformity of nanoparticles, which directly impact drug delivery efficiency and bioavailability. In the case of the F8 optimized formulation, SEM provided valuable insights, as shown in Figure 17. The micrographs of this formulation, identified as L-SNEDDS, revealed oval-shaped crystals with significant drug adsorption on their surfaces. This thorough and consistent drug adsorption highlights the formulation's robustness, suggesting that it has the potential for sustained drug release and improved therapeutic efficacy.

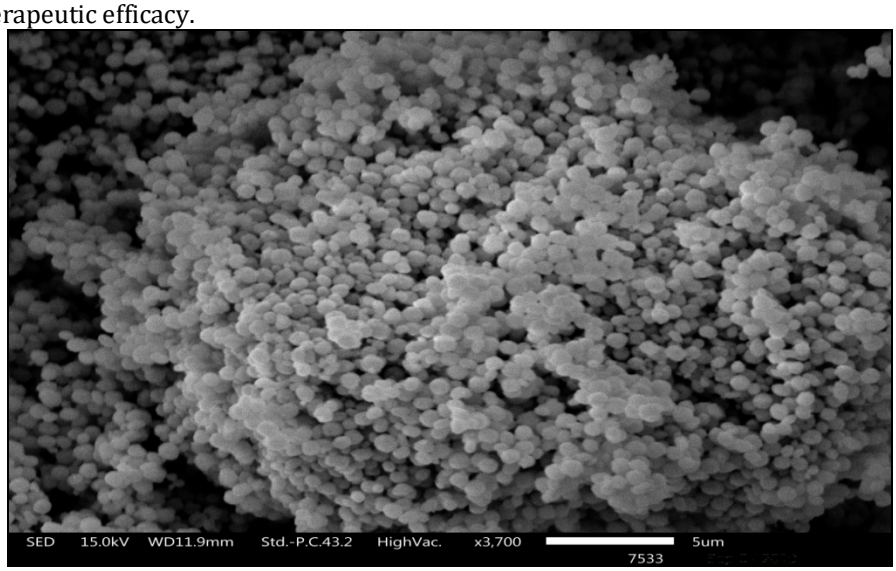

Figure 17: SEM Image of F8 Formulation

TEM

Transmission electron microscopy (TEM) provides an in-depth analysis of the internal structure and fine details of nanoparticles, offering critical information on size, morphology, and the distribution of the drug within the formulation. In the case of the F8 optimized formulation, TEM analysis revealed additional structural insights that complement the SEM findings. The L-SNEDDS formulation displayed distinct oval-shaped crystals, similar to those observed in the SEM micrographs. TEM further illustrated the detailed internal arrangement of these crystals, showcasing the uniformity and homogeneity of drug adsorption on their surfaces as shown in Figure 18. This reinforced the robustness of the formulation, emphasizing its potential for sustained drug release and improved therapeutic efficacy, which is essential for optimizing bioavailability and drug delivery.

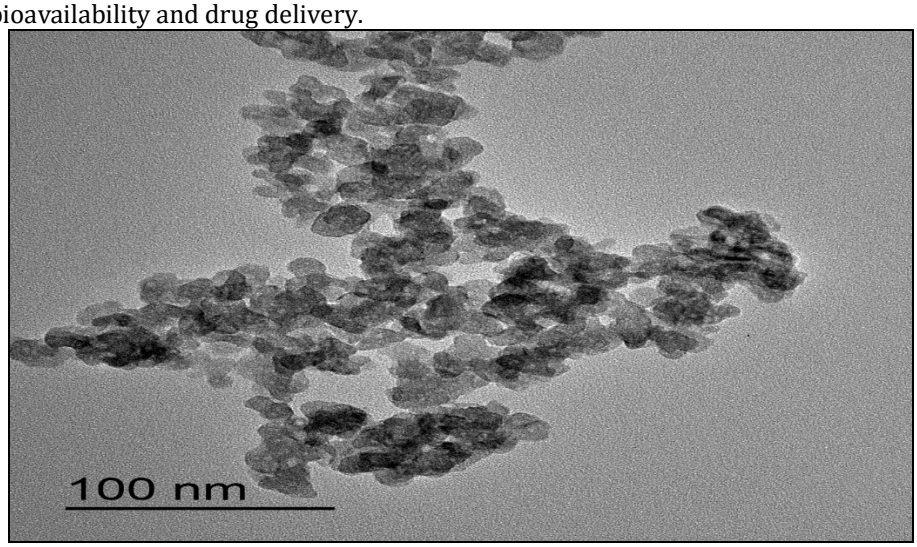

Figure 18: TEM Image of F8 Formulation

Rheological study

The optimized formulation’s refractive index came out to be 152 ± 1.40 cP (Table 10), experiencing the viscous nature of the nanoemulsion.

Table 10: Viscosity and Refractive Index

Batch Code	Viscosity (cP)	Refractive Index
F1	98 ± 1.12	1.433 ± 0.07
F2	112 ± 1.35	1.490 ± 0.09
F3	105 ± 1.26	1.468 ± 0.06
F4	121 ± 1.38	1.512 ± 0.08
F5	115 ± 1.20	1.505 ± 0.10
F6	109 ± 1.30	1.471 ± 0.11
F7	130 ± 1.44	1.620 ± 0.09
F8 (Optimized)	**152 ± 1.40**	**1.752 ± 0.13**
F9	127 ± 1.23	1.590 ± 0.12
F10	103 ± 1.15	1.460 ± 0.08
F11	118 ± 1.27	1.499 ± 0.07
F12	125 ± 1.40	1.580 ± 0.11
F13	99 ± 1.10	1.432 ± 0.06
F14	134 ± 1.36	1.631 ± 0.10
F15	140 ± 1.50	1.702 ± 0.09
F16	110 ± 1.18	1.489 ± 0.08
F17	108 ± 1.22	1.470 ± 0.07
F18	137 ± 1.39	1.689 ± 0.10
F19	101 ± 1.05	1.444 ± 0.09
F20	122 ± 1.30	1.520 ± 0.08

Determination of Refractive Index

The optimized formulation's refractive index came out to be 1.752±0.14 (Table 10), experiencing the isotropy of the nanoemulsion.

***In-vitro* Release Study**

The *in-vitro* drug release from 1,8-Cineole L-SNEDDS of all batches was investigated USP Dissolution Test Apparatus-II (paddle method) from Electrolab, USA. For batches F1-F20, the maximum drug release ranged from approximately 70.69% to 89.64%, as indicated in Table 6&11 and Figure 19. The *in-vitro* release of the formulated 1,8-Cineole L-SNEDDS in phosphate buffer saline (PBS) at pH 7.4 and 37°C was examined, with 1,8-Cineole L-SNEDDS undergoing a 60-minute dialysis. The Optimized L-SNEDDS of F8 achieved a release of more than 75% within just 15min. Therefore, it can be concluded that L-SNEDDS showed optimum dissolution characteristics. The quantity of released drug was assessed using a developed HPTLC method to measure absorbance.

Table 11: *In-vitro* release profile of 1,8-Cineole L-SNEDDS

Sr. No.	Time (Minutes)	1,8-Cineole L-SNEDDS (F8)
1	0	0
2	5	48.31±1.36
3	10	62.55±2.41
4	15	78.84±1.69
5	20	84.53±2.32
6	25	85.67±2.56
7	30	86.42±2.96
8	60	89.83±2.32

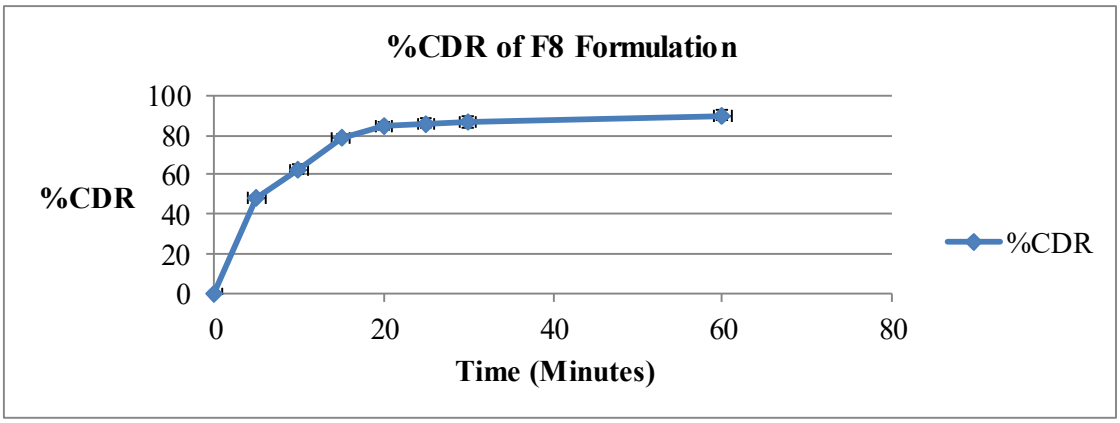

Figure 19: *In-vitro* release profile of F8 Formulation

Stability Study of L-SNEDDS

The thermodynamic stability of the optimized L-SNEDDS formulation was evaluated through rigorous stability tests, including a heating-cooling cycle and centrifugation. Formulations were subjected to six cycles of temperature variation (4°C to 45°C) and centrifugation at 3,500 rpm for 30 minutes to assess their resilience to thermal and mechanical stress. Only formulations that exhibited no signs of instability, such as creaming, cracking, phase separation, or precipitation, were deemed thermodynamically stable. Among the tested formulations, F8 demonstrated exceptional stability, highlighting their robustness and suitability for long-term storage and transportation.

Flow properties S-SNEDDS

Flow properties such as angle of repose, bulk density, tapped density and compressibility index of optimized formulations, and were evaluated to determine the suitability for S-SNEDDS formulation. F8 optimized batch show good flow proprieties and other batches show fair flow properties as shown in Table 12.

Table 12: Pre-Compression Parameters of S-SNEDDS

Batch Code	Bulk Density (gm/ml)	Tapped Density (gm/ml)	Carr's Index (%)	Hausner Ratio	Angle of Repose
F1	0.55 ± 0.03	0.52 ± 0.03	-5.77 ± 0.02	0.95 ± 0.03	23.42 ± 0.20
F2	0.47 ± 0.03	0.55 ± 0.03	14.55 ± 0.02	1.17 ± 0.03	24.58 ± 0.20
F3	0.53 ± 0.03	0.67 ± 0.03	20.9 ± 0.02	1.26 ± 0.03	24.4 ± 0.20
F4	0.52 ± 0.03	0.63 ± 0.03	17.46 ± 0.02	1.21 ± 0.03	24.19 ± 0.20
F5	0.46 ± 0.03	0.62 ± 0.03	25.81 ± 0.02	1.35 ± 0.03	26.33 ± 0.20
F6	0.48 ± 0.03	0.64 ± 0.03	25.0 ± 0.02	1.33 ± 0.03	27.44 ± 0.20
F7	0.49 ± 0.03	0.61 ± 0.03	19.67 ± 0.02	1.24 ± 0.03	24.89 ± 0.20
F8	**0.47 ± 0.03**	**0.59 ± 0.03**	**19.62 ± 0.02**	**1.09 ± 0.03**	**22.95 ± 0.20**
F9	0.57 ± 0.03	0.68 ± 0.03	16.18 ± 0.02	1.19 ± 0.03	24.51 ± 0.20
F10	0.52 ± 0.03	0.62 ± 0.03	16.13 ± 0.02	1.19 ± 0.03	24.42 ± 0.20
F11	0.51 ± 0.03	0.61 ± 0.03	16.39 ± 0.02	1.2 ± 0.03	24.15 ± 0.20
F12	0.51 ± 0.03	0.59 ± 0.03	13.56 ± 0.02	1.16 ± 0.03	26.32 ± 0.20
F13	0.49 ± 0.03	0.61 ± 0.03	19.67 ± 0.02	1.24 ± 0.03	21.41 ± 0.20
F14	0.5 ± 0.03	0.6 ± 0.03	16.67 ± 0.02	1.2 ± 0.03	23.75 ± 0.20
F15	0.48 ± 0.03	0.58 ± 0.03	17.24 ± 0.02	1.21 ± 0.03	24.1 ± 0.20
F16	0.52 ± 0.03	0.63 ± 0.03	17.46 ± 0.02	1.21 ± 0.03	24.65 ± 0.20
F17	0.55 ± 0.03	0.66 ± 0.03	16.67 ± 0.02	1.2 ± 0.03	23.42 ± 0.20
F18	0.49 ± 0.03	0.59 ± 0.03	16.95 ± 0.02	1.2 ± 0.03	25.1 ± 0.20
F19	0.47 ± 0.03	0.57 ± 0.03	17.54 ± 0.02	1.21 ± 0.03	24.9 ± 0.20
F20	0.53 ± 0.03	0.65 ± 0.03	18.46 ± 0.02	1.23 ± 0.03	24.35 ± 0.20

Formulation of Capsule using optimized S-SNEDDS (F8)

Table 13 and 14 showed the formulation table of S-SNEDDS and capsule formulation.

Table 13: Formulation Table for S-SNEDDS (F8)

Sr. No.	Components	Quantity
1	1,8-Cineole	6ml (5520mg)
2	Tween 80	4ml (4240mg)
3	PEG 200	2ml (2240mg)
4.	Mannitol	Q.S.
Total (SNEDDS)		12,000 mg

Tablet 14: Capsule Formulation

Sr. No.	Name of Ingredients	F8 Quantity
1	S-SNEDDS equivalent for 1 Capsule	600mg
Total Weight	600mg	

Evaluation of Capsule

Table 15 presented the evaluation of optimized F8 capsule formation.

Table 15: Evaluation of Capsule containing S-SNEDDS

Batch Code	Uniformity of Content	% Drug content
F8 Cap	0.1789±0.04	96.28±0.022

***In-vitro* dissolution**

The results of *in-vitro* dissolution study of capsules was performed in buffer pH 7.4 and showed that the formulation F8 containing showed ideal release of the drug in 60 minutes as shown in Table 16 and Figure 20.

Table 16: *In-vitro* release profile of F8 Capsule

Sr. No.	Time (Minutes)	Plan Drug	F8 Cap
1	0	0	0
2	5	3.23±0.05	26.33±0.05
3	10	5.79±0.01	47.77±0.09
4	15	7.45±0.04	77.71±0.03
5	20	10.54±0.09	83.39±0.04
6	25	13.37±0.11	87.18±0.06
7	30	16.17±0.06	91.35±0.01
8	60	19.16±0.02	95.90±0.07

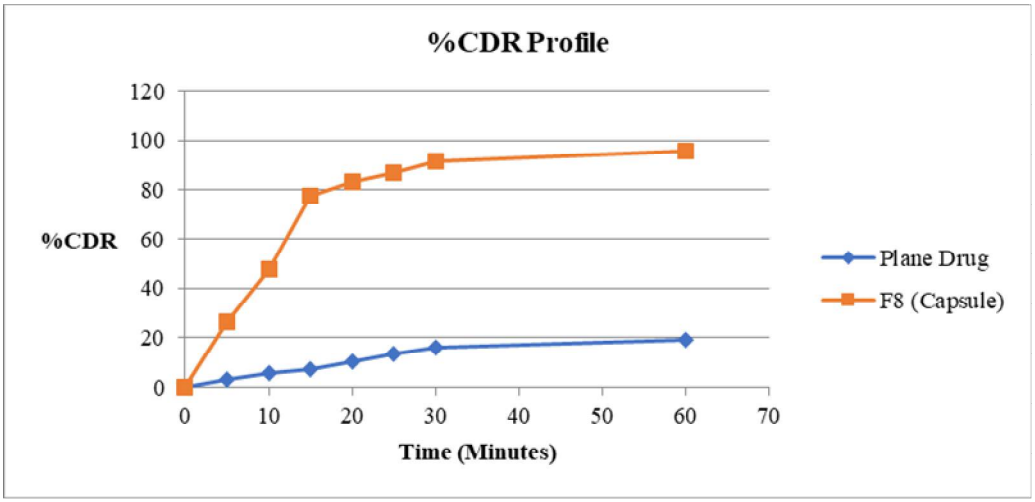

Figure 20: *In-vitro* drug release study F8 Capsule

Stability Study

The optimized capsules were subjected to stability studies and the results are given in Table 17. Based on these results it is revealed that, capsule (Formulation batch **F8**) were found to be stable formulation at the given temperature and humidity condition.

Table 17: Stability study of parameters of the optimized formulation (F8)

Parameters	Initial Month	1st Month	2nd Month	3rd Month
Physical Appearance	No Change			
Drug Content	96.28±0.22	96.12±0.18	96.56±0.22	97.16±0.31
Dissolution (%)	95.90±0.07	96.10±0.10	95.36±0.14	96.84±0.19

CONCLUSION

This research successfully demonstrated the design and development of a novel Self-Nanoemulsifying Drug Delivery System (SNEDDS) for 1,8-Cineole, incorporating both formulation optimization and conversion into a solid dosage form. By addressing the solubility limitations of 1,8-Cineole through lipid-based nanoencapsulation, the study underscores the potential of SNEDDS to overcome the pharmacokinetic barriers associated with poorly water-soluble bioactives. The liquid SNEDDS (L-SNEDDS) formulation was rationally developed using solubility screening, pseudo-ternary phase diagrams, and statistical modeling through Central Composite Design (CCD). This allowed precise control over droplet size, zeta potential, and drug release profiles. The optimized formulation (F8) displayed favorable nano-range particle size, high emulsification efficiency, and uniform dispersion, indicating suitability for oral delivery. Beyond formulation, the study extended into solid-state conversion via lyophilization using mannitol as a cryoprotectant, yielding a free-flowing powder suitable for encapsulation. The resulting Solid SNEDDS (S-SNEDDS) capsules maintained the physicochemical and release characteristics of the liquid formulation, while offering additional benefits such as improved stability, better handling, and ease of dosing. Comprehensive characterization using FTIR, DSC, SEM, and TEM confirmed drug-excipient compatibility and the absence of undesirable interactions or degradation. Flow property analysis, in-vitro dissolution, and 3-month stability testing further validated the robustness of the final capsule formulation. This study not only demonstrates a viable approach to enhance the oral delivery of 1,8-Cineole but also offers a scalable, industry-relevant model for transforming other phytoconstituents or lipophilic drugs into efficient solid oral delivery systems. Future

investigations could explore pharmacokinetic and in-vivo efficacy studies to further substantiate clinical translation and therapeutic benefits of this delivery platform.

REFERENCES

1. Morakul B. (2020). Self-nanoemulsifying drug delivery systems (SNEDDS): An advancement technology for oral drug delivery. Pharm Sci Asia.47(3):205–20.
2. Annisa R, Mutiah R, Yuwono M, Hendradi E. (2023). Nanotechnology Approach-Self Nanoemulsifying Drug Delivery System (Snedds). Int J Appl Pharm. 15(4):12–9.
3. Uttreja P, Youssef AAA, Karnik I, Sanil K, Narala N, Wang H, et al. (2024). Formulation Development of Solid Self-Nanoemulsifying Drug Delivery Systems of Quetiapine Fumarate via Hot-Melt Extrusion Technology: Optimization Using Central Composite Design. Pharmaceutics.16(3).
4. Zingale E, Bonaccorso A, D'Amico AG, Lombardo R, D'Agata V, Rautio J, et al. (2024). Formulating Resveratrol and Melatonin Self-Nanoemulsifying Drug Delivery Systems (SNEDDS) for Ocular Administration Using Design of Experiments. Pharmaceutics. 16(1).190-198
5. Reddy MR, Gubbiyappa KS.(2021). A Comprehensive Review on Supersaturable Self-Nanoemulsifying Drug Delivery System. Asian J Pharm Clin Res. 40–4.
6. Rehman FU, Shah KU, Shah SU, Khan IU, Khan GM, Khan A. (2017). From nanoemulsions to self-nanoemulsions, with recent advances in self-nanoemulsifying drug delivery systems (SNEDDS). Expert Opin Drug Deliv.14(11):1325–40.
7. Mohsin K, Alamri R, Ahmad A, Raish M, Alanazi FK, Hussain MD. Development of self-nanoemulsifying drug delivery systems for the enhancement of solubility and oral bioavailability of fenofibrate, A poorly water-soluble drug. Int J Nanomedicine. 2016;11:2829–38.
8. Farhanghi A, Aliakbarlu J, Tajik H, Mortazavi N, Manafi L, Jalilzadeh-Amin G. Antibacterial interactions of pulegone and 1,8-cineole with monolaurin ornisin against Staphylococcus aureus. Food Sci Nutr. 2022;10(8):2659–66.
9. Juergens LJ, Worth H, Juergens UR. New Perspectives for Mucolytic, Anti-inflammatory and Adjunctive Therapy with 1,8-Cineole in COPD and Asthma: Review on the New Therapeutic Approach. Adv Ther. 2020;37(5):1737–53.
10. Cai ZM, Peng JQ, Chen Y, Tao L, Zhang YY, Fu LY, et al. 1,8-Cineole: a review of source, biological activities, and application. J Asian Nat Prod Res. 2021;23(10):938–54.
11. Hoch CC, Petry J, Griesbaum L, Weiser T, Werner K, Ploch M, et al. 1,8-cineole (eucalyptol): A versatile phytochemical with therapeutic applications across multiple diseases. Biomed Pharmacother. 2023;167.
12. Abbas IK. Self-Nanoemulsifying Drug Delivery System: Liquid, Supersaturable, and Solid Dosage Forms. Al-Rafidain J Med Sci. 2022;3:98–108.
13. Rao MRP, Raut SP, Shirsath CT, Jadhav MB, Chandanshive PA. Self-nanoemulsifying drug delivery system of mebendazole for treatment of lymphatic filariasis. Indian J Pharm Sci. 2018;80(6):1057–68.
14. Møller A, Schultz HB, Meola TR, Joyce P, Müllertz A, Prestidge CA. The Influence of Blonanserin Supersaturation in Liquid and Silica Stabilised Self-Nanoemulsifying Drug Delivery Systems on In Vitro Solubilisation. Pharmaceutics. 2023;15(1).
15. Mhaske NS, Rasane VS. Novel Fast Disintegrating Tablet of Bisoprolol Fumarate with Its Development and Characterization for Patient Compliances. Adv Biores. 2025;16(May):58–64.
16. 16. Pandey S, Shahi S. Characterization of Zinc Nanoparticles from Bija (Pterocarpus marsupium Roxb) Leaf Extract. Adv Biores. 2025;16(July):132–9.
17. Wagh MS, A.J.Dhembare, K.D.Thete3. Study of Anti-Bacterial Activity of Silver Nano Particles from Insulin Plant Costus igneus Against Oral Bacteria in Human ' s. Adv Biores. 2025;16(May):89–94.
18. 18. Deepika V, Naik SS, Charan GV. Preparation and Characterization of Dolutegravir-Loaded BSA Nanoparticles. Adv Biores. 2025;16(July):45–60.
19. Ubarhande YB, Parihar AS. (2025). Comparative Optimization of HPLC Conditions for The Isolation of Caftaric Acid from Ailanthus excelsa using Hydroalcoholic Extraction. Adv Biores.16(July):61–6.
20. Niranjani S, Prema Krishnan, Prabhu S, Gayathri R EE. (2025). Effectualness of Cinnamon , Exercise Programme and Anxiety Reduction Counselling (Multi Interventional Strategies) On Body Mass Index , Waist Circumference and Menstrual Cycle : An Experimental Study Among Young Girls with Polycystic Ovary. Adv Biores. 16(May):58–64.
21. Ukwubile CA, Mathias SN, Pisagih PS. (2025). Acute and Subchronic Toxicity Evaluation and GC-MS Profiling of Ajumbaise: A Traditional Nigerian Polyherbal Formulation for Labor Enhancement and Pain Relief. J Pharm Sci Comput Chem.1(2):154–73.
22. Soumya P, Sofi SI, Vignanandam S, Aishwarya B, Kholi CB, Anusha K, et al. (2025). A Study to Assess the Efficacy of Various Therapeutic Strategies Used in the Treatment of Psoriasis. J Pharm Sci Comput Chem. 2025;1(1):38–49.